REPORT 925

STABILITY DERIVATIVES AT SUPERSONIC SPEEDS OF THIN RECTANGULAR WINGS WITH DIAGONALS AHEAD OF TIP MACH LINES

By Sidney M. Harmon

SUMMARY

Theoretical results are obtained, by means of the linearized theory, for the surface-velocity-potential functions, surface-pressure distributions, and stability derivatives for various motions at supersonic speeds of thin flat rectangular wings without dihedral. The investigation includes steady and accelerated vertical and longitudinal motions and steady rolling, yawing, sideslipping, and pitching for Mach numbers and aspect ratios greater than those for which the Mach line from the leading edge of the tip section intersects the trailing edge of the opposite tip section. The stability derivatives are derived with respect to principal body axes and then transformed to a system of stability axes. In the case of yawing, a treatment for the infinitely long wing which takes account of the spanwise variation in the stream Mach number is extended to the finite wing, and a plausible, although not rigorous, solution is obtained for the wing tip effects.

The results for this investigation showed that positive yawing at supersonic speeds may produce a negative rolling moment in contrast to the behavior at subsonic speeds where a positive rolling moment would be produced. The attainment of supersonic speed should produce a significant change in the positive direction of the yawing moment per unit rolling velocity. The results also indicate that unstable tendencies are produced by vertical accelerations if

$$A\sqrt{M^2-1} \geqq \frac{M^2+1}{3}$$

where A is wing aspect ratio and M is stream Mach number.

INTRODUCTION

Recent developments in supersonic airfoil theory (references 1 to 4) have led to the calculation of many of the supersonic stability derivatives for various plan forms. In references 5 to 8, various theoretical supersonic stability derivatives for small disturbances are presented for thin flat wings of delta plan form. In reference 9, the supersonic damping due to rolling is given for triangular, trapezoidal, and related plan forms.

In the present paper the methods of references 4, 10, and 11, which are based on the linearized theory for a uniform stream Mach number, are used to derive the supersonic surface-velocity-potential functions for thin flat rectangular wings without dihedral in steady and accelerated vertical motions and steady rolling, sideslipping, and pitching motions. The potential functions that are obtained are then used to derive formulas for the pressure distributions and the stability derivatives for the foregoing motions and also for steady yawing. In the case of yawing, a simple treatment given in reference 7 for the infinitely long wing, which takes account of the spanwise variation in stream Mach number associated with yawing, has shown that the assumption of a uniform Mach number is far from adequate to describe the compressibility effects. This treatment is extended herein in order to evaluate the wing tip effects for the yawing finite-span wing.

The steady motions that are treated herein are assumed to give small deviations from the undisturbed flight path and the accelerated motions are assumed to have small accelerations. Theoretical results based on this assumption for steady motions have, in general, been found to be reliable; however, the reliability of such results for unsteady motions is as yet unverified. The results presented herein cover a range of Mach number and aspect ratio greater than that for which the Mach line from the leading edge of the tip section intersects the trailing edge of the opposite tip section.

SYMBOLS

x,y	rectangular coordinates (see fig. 1)
u_0,v_0	induced flow velocities along x- and y-axes, respectively
l	coordinate in flight direction if this direction is inclined to x-axis
u,v,w	incremental flight velocities along x-, y-, and z-axes, respectively (see fig. 2)
$\dot{u}$	derivative of u with respect to time
$\dot{w}$	accelerated vertical motion
V	undisturbed flight velocity
V'	local flight velocity after disturbance; used to indicate inclination of flight direction to x-axis (see fig. 1)
p,q,r	angular velocities about x-, y-, and z-axes, respectively (see fig. 2)
a	speed of sound
M	stream Mach number (V/a)
$B=\sqrt{M^2-1}$	
μ	Mach angle $\left(\sin^{-1}\frac{1}{M}\right)$
α	wing angle of attack in steady flight, radians (w/V)
α'	local inclination of airfoil surface with respect to free stream, radians $\left(\frac{w}{V+u}\right)$

$\dot{\alpha}$	derivative of α with respect to time
t	time following disturbance, seconds
β	angle of sideslip, radians (v/V)
c	chord
h	wing semispan
b	wing span
S	total wing area
S_w	region of integration over portion of wing surface (see fig. 3)
A	aspect ratio $\left(\dfrac{2h}{c}\text{ or }\dfrac{b}{c}\right)$
x_{os}	distance of origin of stability axes from the midchord point, measured along x-axis, positive ahead of midchord point
ρ	mass density of air
ϕ	disturbance-velocity potential on upper surface of airfoil
ξ,η	auxiliary variables which replace x and y, respectively (see fig. 1)
y_a,η_a	indicates a transformation of origin of x- and y-axes or ξ- and η-axes from leading edge of center section to leading edge of tip section $(y_a=y-h$ on right half-wing; $y_a=-y-h$ on left half-wing)
ΔP	pressure difference between lower and upper surfaces of airfoil, positive in direction of lift
Δc_P	nondimensional coefficient expressing ratio of pressure difference between lower and upper surfaces of airfoil to free-stream dynamic pressure $\left(\dfrac{\Delta P}{\frac{\rho}{2}V^2}\right)$
G	constant given by equation (9)
F_s	induced suction force on wing tip per unit length of tip
X,Y,Z	forces parallel to x-, y-, and z-axes, respectively (see fig. 2)
C_X	longitudinal-force coefficient $\left(\dfrac{X}{\frac{\rho}{2}V^2S}\right)$
C_Y	lateral-force coefficient $\left(\dfrac{Y}{\frac{\rho}{2}V^2S}\right)$
C_Z	vertical-force coefficient $\left(\dfrac{Z}{\frac{\rho}{2}V^2S}\right)$
C_{D_0}	skin-friction drag coefficient $\left(\dfrac{\text{Skin-friction drag}}{\frac{\rho}{2}V^2S}\right)$
L,M,N	moments about x-, y-, and z-axes, respectively (see fig. 2); M is also used to refer to Mach number

C_l	rolling moment coefficient $\left(\dfrac{L}{\frac{\rho}{2}V^2Sb}\right)$
C_m	pitching-moment coefficient $\left(\dfrac{M}{\frac{\rho}{2}V^2Sc}\right)$
C_n	yawing-moment coefficient $\left(\dfrac{N}{\frac{\rho}{2}V^2Sb}\right)$

Subscript:

1,2 contributions of normal pressures and skin friction, respectively, to C_{x_r}; also used to indicate component parts of C_{l_β}, $C_{z_{\dot{\alpha}}}$, $C_{m_{\dot{\alpha}}}$, C_{z_u}, and C_{m_u}

Superscript:

w,p contributions caused by vertical motion and rolling motion, respectively

Whenever p, q, r, β, α, u, $\dot{\alpha}$, and $\dot{u}$ are used as subscripts, a nondimensional derivative is indicated and this derivative is the slope through zero. For example:

$$C_{l_p}=\left[\frac{\partial C_l}{\partial\left(\frac{pb}{2V}\right)}\right]_{p\to0}\qquad C_{m_\alpha}=\left(\frac{\partial C_m}{\partial\alpha}\right)_{\alpha\to0}$$

$$C_{m_q}=\left[\frac{\partial C_m}{\partial\left(\frac{qc}{2V}\right)}\right]_{q\to0}\qquad C_{m_u}=\left[\frac{\partial C_m}{\partial\left(\frac{u}{V}\right)}\right]_{u\to0}$$

$$C_{l_r}=\left[\frac{\partial C_l}{\partial\left(\frac{rb}{2V}\right)}\right]_{r\to0}\qquad C_{m_{\dot{\alpha}}}=\left[\frac{\partial C_m}{\partial\left(\frac{\dot{\alpha}c}{2V}\right)}\right]_{\dot{\alpha}\to0}$$

$$C_{l_\beta}=\left(\frac{\partial C_l}{\partial\beta}\right)_{\beta\to0}\qquad C_{m_{\dot{u}}}=\left[\frac{\partial C_m}{\partial\left(\frac{\dot{u}c}{V^2}\right)}\right]_{\dot{u}\to0}$$

Unprimed stability derivatives refer to principal body axes; primed stability derivatives refer to stability axes.

ANALYSIS

GENERAL CONCEPTS

The coordinate axes and the symbols used in the analysis of the rectangular wing are shown in figure 1. The derivation of the formulas for the surface-velocity-potential functions, pressure distributions, and stability derivatives is made initially with reference to principal body axes which are fixed in the wing with the origin at the midchord of the center section $\left(\dfrac{c}{2},0,0\right)$. This system of axes is shown in figure 2 (a). The transformation of these stability derivatives to a system of stability axes (fig. 2 (b)) is discussed in the section entitled "Results and Discussion."

The stability derivatives are determined from integrations of the forces and moments over the wing. For vertical and
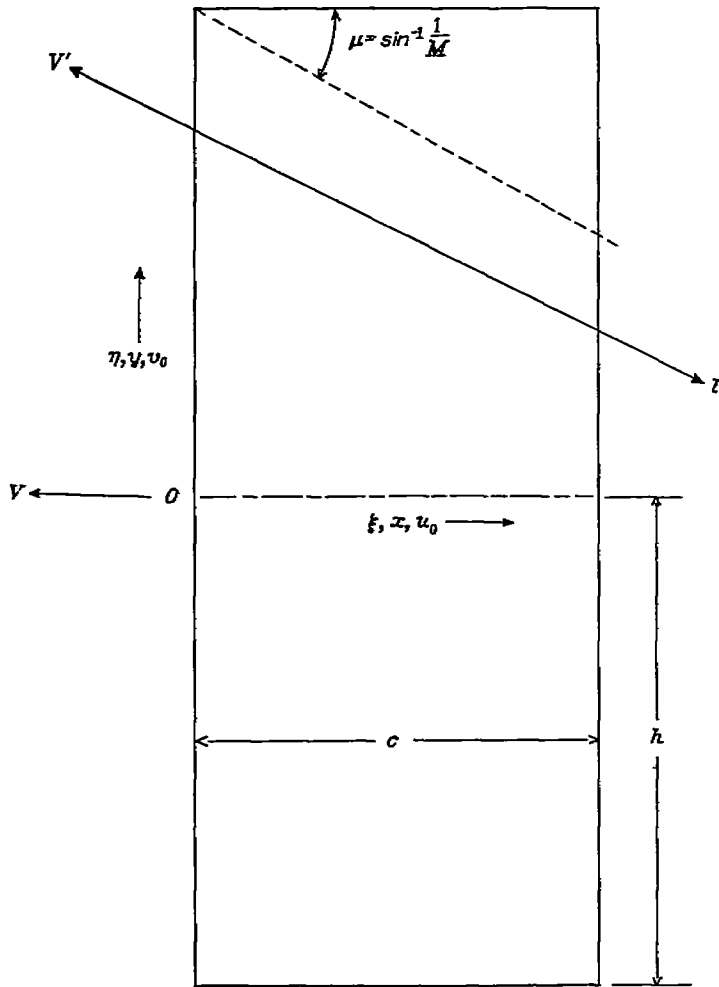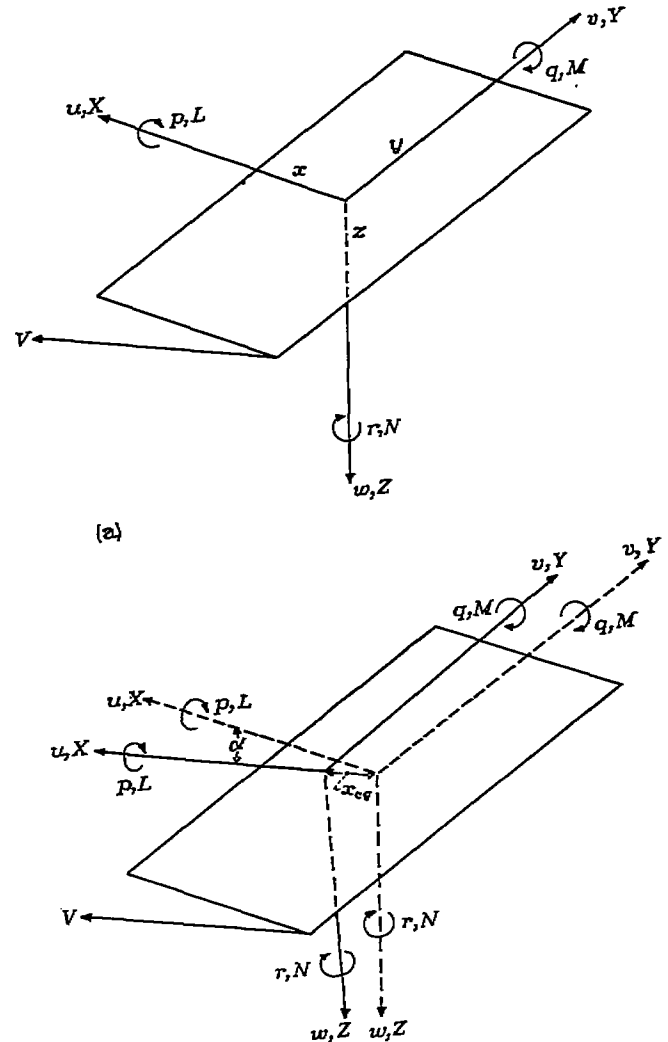
FIGURE 1.—Axes and notation used in analysis.

(a)

(b)

(a) Principal body axes. Origin at center of wing.

(b) Stability axes. Origin at point $\left(\frac{c}{2}-x_{eg},0,0\right)$.

Principal body axes dotted for comparison.

FIGURE 2.—Velocities, forces, and moments relative to principal body and stability axes.

pitching motions which yield equal and opposite suction forces along the edge of each wing tip, the only resultant forces and moments acting on the wing, if skin friction is neglected, are those caused by the pressures on the airfoil surfaces. These pressures are obtained from the familiar Bernoulli equation. In rolling, yawing, or sideslipping, however, unbalanced suction forces which produce lateral forces and yawing moments are induced along the wing tips in addition to the forces and moments resulting from the pressure normal to the wing surface. The subsequent analysis for the calculation of the stability derivatives is then resolved to a determination of the pressure distribution normal to the surface and the unbalanced suction forces along the wing-tip edges.

The pressure difference between the upper and lower surfaces (positive upward) at any point on the wing is determined from the general Bernoulli equation for small disturbances as

$$\Delta P = 2\rho \left(V'' \frac{\partial \phi}{\partial l} + \frac{\partial \phi}{\partial t} \right) \qquad (1)$$

where V'' is the local flight velocity and l refers to a coordinate measured in the flight direction. The term $\partial \phi/\partial t$ expresses the effect of any unsteadiness in the flow. The velocity potential ϕ in equation (1) must be determined so as to satisfy the linearized partial-differential equation (with time dependency if the motion is unsteady) of the flow and the boundary conditions associated with the particular motion under consideration. Thus, the potential must give streamlines that are tangent to the airfoil surface and a pressure field that is continuous at all points exterior to the wing. Equation (1) shows that the pressure distribution on the wing is determined when the surface-potential function is found.

The method of reference 4 is in general adaptable to the problem of obtaining the surface-potential function ϕ in supersonic flight to meet boundary conditions associated with small

steady motions, such as vertical motions, rolling, sideslipping, and pitching. The method is an extension, to include tip effects, of the work of Puckett and others which uses the superposition of elementary source solutions to obtain the potential function. In cases where a point on the wing is influenced by two or more mutually interacting external fields, the interaction introduces difficulties in the solution for the surface potential. (See also reference 12.) If any point on the wing is influenced by only one independent external field, however, the potential function in a region affected by the wing tip may be obtained by integration of elementary source solutions solely over an appropriate area of the wing. The strength of these sources is shown to be a function only of the local slope of the airfoil surface with reference to the free-stream direction. Inasmuch as the slope of the airfoil surface with reference to the free-stream direction is known for a given motion, the distribution of sources is known and, consequently, the distribution of the surface-potential function is determined by an integration of the elementary source solutions over an appropriate area of the wing.

As applied to the rectangular wing at supersonic speeds, the foregoing method of reference 4 for one independent external field is valid as long as the foremost Mach wave from one tip does not intersect the opposite tip, that is, for Mach numbers and aspect ratios for which $AB \geqq 1$. For this case, the potential at a point on the top surface of a thin flat wing may be determined by means of equation (14) of reference 4 and is as follows:

$$\phi(x,y_a) = \frac{V}{\pi} \int \int_{S_w} \frac{\alpha' \, d\xi \, d\eta_a}{\sqrt{(x-\xi)^2 - B^2(y_a - \eta_a)^2}} \qquad (2)$$

where α' represents the local angle of attack of the airfoil surface at the point (ξ, η_a). Figure 3 shows a typical region S_w for determining the potential at a point (x,y_a) in a rectangular wing. The figure shows the boundaries S_w over which the integration must be performed, for a point (x,y_a) which is affected by the wing-tip region. If the point (x,y_a) is located at or inboard of the foremost Mach line from the tip, this point is unaffected by the tip region and S_w is bounded by the leading edge and the Mach forecone from (x,y_a). Suppose that the surface potential $\phi(x,y)$ has been obtained from equation (2) or by some other method, then the differentiation of ϕ with respect to the coordinate in the free-stream direction determines the pressure distribution by means of the Bernoulli relation, equation (1).

The expressions for determining the surface potential and the pressure coefficient for unsteady motions are discussed in the section entitled "Derivation of Formulas."

DERIVATION OF FORMULAS

The subsequent derivation of formulas for the various motions will involve first the determination of distributions of surface potential and then the determination of surface-pressure distributions and any unbalanced suction forces along the wing tips. The integrals required for these derivations and also those required for the stability derivatives are integrable either directly or after reduction by parts by means of standard formulas such as are given in reference 13; hence, the details for the integrations are not shown. In the operations involving factoring from radicals, care must be used to preserve the correct sign of the factors; for example, if

$$y_a < 0$$

then

$$\sqrt{y_a^2} = \sqrt{(-y_a)^2} = -y_a$$

For brevity, the final formulas are omitted from the derivations and appear only in tables at the end of the paper. Thus, the distributions of ϕ and Δc_P are summarized in table I, and the stability derivatives are summarized in table II.

All the derivations are made specifically for a wing for which $AB \geqq 2$, that is, for which the foremost Mach wave from a tip does not intersect the remote half-wing. The formulas in table I for the potential ϕ and pressure coefficient Δc_P that are obtained for $AB \geqq 2$ can be applied to wings in which $1 \leqq AB \leqq 2$ by using the principle of symmetry and superposing separately each tip effect at the point under consideration to the value obtained for the infinitely long wing. A consideration of this superposition principle for the rectangular wing shows, however, that the stability derivatives which are obtained for $AB \geqq 2$ apply as well to wings for which $AB \geqq 1$. A more detailed description of table II is given in the section entitled "Results and Discussion."

VERTICAL, PITCHING, AND LONGITUDINAL MOTIONS

Derivatives $-C_{z_\alpha}$ and $-C_{z_q}$.—For steady pitching motion about a lateral axis through the midchord point, the local slope of the airfoil surface with respect to the free-stream direction is

$$\alpha' = \alpha + \frac{\left(\xi - \frac{c}{2}\right)}{V} q$$

where α is the angle of attack in the absence of pitching. In order to obtain the potential distribution, this value of α' is substituted into equation (2) and the double integration for the variables ξ and η_a is performed between the limits indicated in figure 3. The pressure coefficient is then obtained from equation (1) for steady motions as

$$\Delta c_P = \frac{4}{V} u_0 = \frac{4}{V} \frac{\partial \phi}{\partial x} \qquad (3)$$

These pressure coefficients are then differentiated with respect to α and q. The integrations of the respective distributions of Δc_P over the wing and conversion to nondimensional units then give the derivatives $-C_{z_\alpha}$ and $-C_{z_q}$.

FIGURE 3.—Region of integration for obtaining supersonic velocity-potential function for rectangular wing of finite wing span. Region of integration for point (x, y_a) shown cross-hatched; $y_a = y - k$ on right half-wing; $y_a = -y - k$ on left half-wing.

Derivatives C_{m_α} and C_{m_q}.—Derivatives C_{m_α} and C_{m_q} are obtained directly from the pressure-coefficient distributions for angle of attack and pitching, thus

$$C_m = \frac{1}{hc^2} \int_{-h}^{0} \int_{0}^{c} \Delta c_P \left(\frac{c}{2} - x\right) dx \, dy_a$$

where Δc_P for angle of attack and pitching is given in table I.

Derivatives C_{X_α} and C_{X_q}.—At supersonic speeds the resultant pressure force on a rectangular wing of zero thickness acts normal to the surface as there is no suction at the leading edge. Thus, the forces in the x-direction arise solely from skin friction. On the assumption that the skin friction is independent of α and q, the derivatives C_{X_α} and C_{X_q} are zero.

Derivatives $-C_{Z_u}$, C_{m_u}, and $-C_{X_u}$.—The derivative $-C_{Z_u}$ is obtained from the equation

$$-Z = -\alpha' C_{Z_\alpha} \frac{\rho}{2} (V+u)^2 S$$

Then

$$-C_{Z_u} = \frac{1}{V} \frac{\partial}{\partial u} [-\alpha' C_{Z_\alpha} (V+u)^2]_{u \to 0}$$

The function $-C_{Z_\alpha}$ is obtained from table II. Its dependence on the incremental flight velocity U is indicated by giving B in the form $\sqrt{\dfrac{(V+u)^2}{a^2} - 1}$ and α' in the form $\dfrac{w}{V+u}$. Then

$$-C_{Z_u} = \frac{1}{V} \frac{\partial}{\partial u} \left[\frac{4w(V+u)}{\sqrt{\frac{(V+u)^2}{a^2} - 1}} \left(1 - \frac{1}{2A\sqrt{\frac{(V+u)^2}{a^2} - 1}}\right) \right]_{u \to 0}$$

The derivative C_{m_u} is obtained from the equation

$$M = \alpha' C_{m_\alpha} \frac{\rho}{2} (V+u)^2 Sc$$

Then

$$C_{m_u} = \frac{1}{V} \frac{\partial}{\partial u} [\alpha' C_{m_\alpha} (V+u)^2]_{u \to 0}$$

The function C_{m_α} is obtained from table II, where its dependence on u is indicated by writing α' and B in the same form given previously for the derivative $-C_{Z_u}$. Then

$$C_{m_u} = \frac{1}{V} \frac{\partial}{\partial u} \left\{ \frac{w(V+u)}{3A\left[\frac{(V+u)^2}{a^2} - 1\right]} \right\}_{u \to 0}$$

The derivative $-C_{X_u}$ results from skin friction and is obtained from the equation

$$-X = C_{D_0} \frac{\rho}{2} (V+u)^2 S \cos \alpha$$

Then

$$-C_{X_u} \approx \frac{1}{V} \frac{\partial}{\partial u} [C_{D_0} (V+u)^2]_{u \to 0}$$

ACCELERATED MOTIONS

For accelerated motions in the vertical plane of symmetry, the pressure coefficient from equation (1) is

$$\Delta c_P = \frac{4}{V} \left(\frac{\partial \phi}{\partial x} + \frac{1}{V} \frac{\partial \phi}{\partial t}\right) \tag{4}$$

The surface potential ϕ in equation (4) for unsteady motions of thin airfoils in two-dimensional supersonic flow has been derived in reference 14. In reference 10, the methods of references 4 and 12 for steady flow at supersonic speeds are extended in order to determine solutions for the surface potential and pressure coefficient for unsteady motions in three-dimensional flow. In the present analysis the solutions obtained in reference 10 will be utilized to calculate the derivatives in vertical motions with small constant accelerations.

Derivatives $-C_{Z_{\dot\alpha}}$, $C_{m_{\dot\alpha}}$, and $-C_{X_{\dot\alpha}}$.—The surface potential ϕ for uniformly accelerated motion as obtained for the region within the tip Mach cone is (reference 10, equation (31))

$$\phi(x, y_a) = \frac{1}{B\pi} \left\{ \left[2BV\dot\alpha t + \frac{M^2 \dot\alpha (2y_a B - x)}{3B} \right] \sqrt{-y_a \left(y_a + \frac{x}{B}\right)} + \left(V\dot\alpha tx - \frac{M^2 \dot\alpha x^2}{2B^2}\right) \cos^{-1}\left(\frac{2y_a B}{x} + 1\right) \right\} \tag{5}$$

In converting from the notation of reference 10 for a rectangular wing to the present notation, the following transformations are made: $U = V$, $m = \dot\alpha$, $\alpha = 0$, $\beta = B$, $c = \dfrac{V}{M}$, $k_1 = 1$, $u_2 = v_w = \dfrac{M}{2B}(x + y_a B)$, $u_w = \dfrac{M}{2B}(x - y_a B)$, $\dfrac{du_2}{dv_w} = 1$, and

$C_p = -\dfrac{\Delta c_P}{2}$. In order to obtain ϕ in the region between the tip

Mach cones, y_a in equation (5) is set equal to $-\dfrac{x}{B}$ and, therefore,

$$\phi = \frac{V}{B}\left(\dot\alpha t x - \frac{M^2 \dot\alpha x^2}{2B^2 V}\right) \tag{6}$$

The pressure coefficient Δc_P contributed by the vertical accelerating motion is obtained by partial differentiation of ϕ (equations (5) and (6)) with respect to x and t, by letting $t=0$, and then by substituting these expressions for $\partial\phi/\partial x$ and $\partial\phi/\partial t$ in equation (4). This process yields in the region within the tip Mach cones

$$\Delta c_P(x,y_a) = \frac{4\dot\alpha}{\pi B^2 V}\left[-\frac{x}{B}\cos^{-1}\left(\frac{2y_a B}{x}+1\right) + 2B^2\sqrt{-y_a\left(y_a+\frac{x}{B}\right)}\right] \tag{7}$$

and in the region between the tip Mach cones

$$\Delta c_P = -\frac{4\dot\alpha x}{VB^3} \tag{8}$$

Equations (7) and (8) correspond to equation (33) of reference 10, after the appropriate transformations noted previously for ϕ are made.

The derivatives $-C_{z_{\dot\alpha}}$ and $C_{m_{\dot\alpha}}$ are then obtained by integration of the corresponding Δc_P-distributions and conversion to nondimensional units. The derivative $C_{x_{\dot\alpha}}$ is shown to be zero by the use of assumptions similar to those noted previously for C_{x_α}.

Derivatives $-C_{z_{\dot u}}$, $C_{m_{\dot u}}$, and $-C_{x_{\dot u}}$.—For small accelerations along the flight path, the potential will remain substantially unchanged. The increments in pressure caused by these accelerations, therefore, are assumed to be negligible, and the derivatives $-C_{z_{\dot u}}$, $C_{m_{\dot u}}$, and $-C_{x_{\dot u}}$ are approximately zero.

ROLLING

Derivative C_{l_p}.—In steady rolling motion with angular velocity p, the local slope of the airfoil surface with respect to the flow direction is

$$\alpha' = \frac{p\eta}{V} = \frac{p(\eta_a + h)}{V}$$

In order to obtain the potential distribution this value of α' is substituted into equation (2) and the double integration for the variables ξ and η_a is performed between the limits indicated in figure 3. The pressure coefficient is then obtained from equation (3). The derivative C_{l_p} is obtained by integrating the moments of the Bernoulli pressure distribution for rolling given in table I and by converting this result to coefficient form.

Derivatives C_{Y_p} and C_{n_p}.—In a rolling motion, the lateral force and yawing moment relative to body axes result entirely

from suction along the tips. These suction forces may be evaluated by applying a method suggested in reference 15 for incompressible flow and modified for compressibility effects in reference 3. Thus, if the induced surface velocity normal to the wing tip is expressed as

$$v_0 = \pm\frac{G}{\sqrt{-y_a}} \tag{9}$$

where G is a constant, then the suction force per unit length of tip is

$$F_S = \pi\rho G^2$$

(A more general expression for edge suction that is still valid when the edge is inclined to the stream is given in reference 3 and recast in reference 7.)

Consider the induced surface velocity normal to the tip of a wing rolling with an initial angle of attack α. This velocity is

$$(v_0)^{w+p} = \frac{\partial\phi}{\partial y} = \left(\frac{\partial\phi}{\partial y}\right)^w + \left(\frac{\partial\phi}{\partial y}\right)^p$$

where the superscripts w and p refer to the potentials obtained for a vertical motion and a rolling motion, respectively. From table I

$$\phi^w(x,y_a) = \frac{V\alpha}{\pi}\left[\frac{x}{B}\cos^{-1}\left(\frac{2y_a B}{x}+1\right) + 2\sqrt{-y_a\left(y_a+\frac{x}{B}\right)}\right]$$

and partial differentiation of ϕ^w with respect to y yields

$$(v_0)^w = \left(\frac{\partial\phi}{\partial y}\right)^w = \left(\frac{\partial\phi}{\partial y_a}\right)^w = -\frac{2V\alpha}{\pi}\sqrt{-1-\frac{x}{y_a B}} \tag{10}$$

where $y_a < 0$. Very near the tip, $-y_a \to 0$ and

$$(v_0)^w = \left(\frac{\partial\phi}{\partial y}\right)^w = -\frac{2V\alpha}{\pi}\sqrt{\frac{x/B}{-y_a}} \tag{11}$$

The potential in rolling ϕ^p is given in table I. By partial differentiation of ϕ^p with respect to y and then by letting $-y_a \to 0$, there results

$$(v_0)^p = \frac{\partial\phi}{\partial y_a} = -\frac{2p}{\pi}\sqrt{\frac{x}{B}}\left(\frac{h-\frac{x}{3B}}{\sqrt{-y_a}}\right) \tag{12}$$

The resultant induced surface velocity normal to the wing tip as $-y_a \to 0$ is obtained by adding equations (11) and (12). Thus

$$(v_0)^{w+p} = -\frac{2}{\pi}\sqrt{\frac{x}{B}}\left[\frac{p\left(h-\frac{x}{3B}\right)\pm V\alpha}{\sqrt{-y_a}}\right] \tag{13}$$

The plus sign before V refers to the right wing tip and the negative sign refers to the left wing tip.

Very near the wing tip, equation (13) has the same form as equation (9) and, therefore, the total suction force per unit length along the wing tip is

$$F_s = \pi \rho G^2 = \frac{4\rho x}{\pi B}\left[p^2\left(h - \frac{x}{3B}\right)^2 \pm 2pV\alpha\left(h - \frac{x}{3B}\right) + V^2\alpha^2 \right] \tag{14}$$

In equation (14) only the term $\pm\frac{8\rho x p V\alpha}{\pi B}\left(h - \frac{x}{3B}\right)$ will give rise to a lateral force and a yawing moment which are obtained by integrating this term along the wing tips. These forces and moments are then converted to non-dimensional form to give the derivatives C_{Y_p} and C_{n_p}.

SIDESLIP

The pressure coefficient obtained from equation (1) for steady flight is

$$\Delta c_P = \frac{4}{V'}\frac{\partial\phi}{\partial l}$$

where V' and l are measured in the flight direction. If sideslip occurs the flight direction is inclined relative to the x-axis by the sideslip angle β. The rectangular wing in sideslip, therefore, becomes equivalent to a yawed wing with the leading wing tip raked out and the trailing wing tip raked in. If the Kutta-Joukowski condition at the trailing wing tip is neglected, the potential function for the yawed rectangular plan form may be obtained by the method of reference 4. In reference 11, the method of reference 4 is extended in order to obtain solutions for edges for which the Kutta-Joukowski requirement must be satisfied.

Physical considerations suggest, however, that for small sideslip angles, the actual flow for typically rounded wing tips would in general be unlikely to conform to the Kutta-Joukowski conditions along the trailing wing tip. The edge suction for a lifting wing arises because of the flow from the bottom surface to the top surface around the side edge. This flow may be presumed to go around any boundary layer that may be present. The local boundary layer thus experiences the edge suction. Rough calculations suggest that the edge suction per unit area is approximately constant from the leading edge to the point of maximum profile thickness, and then increases rapidly from the point of maximum thickness to the trailing edge. The pressure gradient is therefore favorable and the flow at the side edge is not expected to separate. This condition should persist for small or moderate amounts of sideslip until the additional pressure increment caused by sideslip produces a strong adverse pressure gradient. Further theoretical and experimental investigation is required to obtain quantitative results regarding these phenomena. On the basis of the foregoing considerations, it will be assumed in the present analysis that the Kutta-Joukowski condition is not satisfied along the trailing wing tip. The effect of satisfying the Kutta-Joukowski condition along the trailing wing tip in sideslip is discussed in this analysis and also in the section entitled "Results and Discussion."

Derivative C_{l_β}.—The potential corresponding to a thin rectangular wing at an angle of attack and a finite angle of sideslip may be obtained from reference 4, equation (20). The corresponding pressure distribution may be obtained from reference 11, appendix C, equation (C4). These solutions from references 4 and 11 were simplified to the approximate form for small angles of sideslip ($\beta^2 \ll 1$) and converted to the present notation with respect to axes shown in figure 1. The distributions for ϕ and Δc_P caused by combined vertical motion and sideslip are given in table I. The regions for which these expressions for ϕ and Δc_P are applicable are bounded by Mach lines with respect to the stream velocity V' which is inclined to the x-axis by the sideslip angle β. As noted previously, these expressions do not satisfy the Kutta-Joukowski condition along the trailing wing tip. As indicated in reference 11, however, the Kutta-Joukowski condition along the trailing wing tip merely cancels the radical term in the expression for Δc_P within the Mach cone from the trailing wing tip.

A consideration of the foregoing Δc_P-distributions indicates that as a result of sideslip the lift within the Mach cone from the leading wing tip is increased, whereas the lift within the Mach cone from the trailing wing tip is decreased. A rolling moment is thereby produced. Furthermore, as a result of sideslip, the Mach lines are shifted toward the trailing wing tip, and this shift contributes an additional rolling moment. The magnitude of the rolling moment caused by sideslip is given in table II in terms of the nondimensional derivative $(C_{l_\beta})_{\beta \to 0}$.

Derivatives C_{Y_β} and C_{n_β}.—The derivatives C_{Y_β} and C_{n_β} can result solely from suction forces which are induced at the wing tips. These suction forces for sideslipping motion were evaluated by a method similar to that described previously for obtaining C_{Y_p} and C_{n_p}. The treatment for sideslip was based on the conclusion, noted previously, that the Kutta-Joukowski condition is unlikely to be satisfied for typically rounded wing tips at small angles of sideslip. The potential ϕ for determining the induced velocity normal to the wing tip was obtained from table I. The resultant lateral force and yawing moment are given in nondimensional form in table II.

YAWING

In yawing flight, the stream velocity varies linearly along the span. This effect introduces variations of both dynamic pressure and compressibility effects along the wing span. The surface potential as expressed in equation (2) satisfies the linearized potential equation for a uniform stream Mach number, but is inadequate to account for the compressibility effects associated with a spanwise variation of stream Mach number. (See reference 7.) The case of the trapezoidal wing with tips cut off along the Mach lines (raked tips) was analyzed in reference 7. It was shown that the pressure distribution could be obtained by application of the Ackeret two-dimensional theory modified by using the local Mach number at each spanwise station as affected by the yawing.

Inclusion of the spanwise variation in Mach number was demonstrated to have a profound effect on the pressure distribution.

The addition of suitable triangular tips to the aforementioned trapezoidal wing converts it into a rectangular wing. The added tips lie wholly within the tip Mach cones and thus their addition does not alter the pressures on the trapezoidal portions. A rigorous solution for the pressures on the tip portions cannot yet be demonstrated. However, an expression that appears plausible has been obtained. This pressure distribution for the tip portions is derived by superposing on the Ackeret pressure distribution, as modified by local Mach number, an appropriate function which fulfills the boundary condition for no pressure discontinuities in the region exterior to the wing. This function thus represents the effect of the wing cut-off and is designated herein as the tip effect. The pressure difference ΔP at any point according to the Ackeret theory based on local Mach number is (reference 7):

$$(\Delta P)_{A-\infty} = \frac{2\rho(V-ry)w}{\sqrt{\left(\frac{V-ry}{a}\right)^2 - 1}} \approx \frac{2\rho w V}{B}\left(1 + \frac{ry}{B^2 V}\right) \quad (15)$$

Equation (15) shows that the pressure distribution for an infinitely long wing which has a steady yawing velocity r and vertical velocity w is expressed by two components. One of these components is proportional to w, is constant, and gives the pressure distribution contributed by an angle of attack in straight flight. The other component is proportional to wr, gives a linear antisymmetrical distribution with respect to y, and expresses the pressure distribution contributed by yawing.

It will be recalled that the solution for steady rolling, treated in a preceding section, resulted likewise in a pressure distribution proportional to y in the region between the tip Mach cones. The pressure distributions contributed by rolling and by yawing are thus proportional in the region between the tip Mach cones. The wing cut-off is effected by canceling the disturbance pressures outboard of the desired tip location by means of a function that satisfies the boundary conditions on the wing. Because the two pressure distributions to be canceled correspond in the yawing and rolling cases, the incremental pressure function or tip effect for each case evidently must reduce to forms which will have the same factor of proportionality in the entire plane of the wing outboard of the tip. It seems reasonable to assume, therefore, that for small yawing motions the two pressure distributions will also have very nearly the same factor of proportionality within the tip Mach cones.

The proportionality constant between the pressure distributions for rolling and yawing motions may be determined by a comparison of the cases of rolling and yawing in column 4 of table I. The pressure coefficient per unit yawing velocity is seen to be α/B^2 times the pressure coefficient per unit rolling velocity, or

$$(\Delta c_P)_{yawing} = \frac{\alpha r}{B^2 p}(\Delta c_P)_{rolling} \quad (16)$$

where equation (16) will apply over the whole wing.

Derivative C_{l_r}.—The preceding analysis indicated that the pressure distribution per unit yawing velocity is in a simple ratio to that produced per unit rolling velocity (equation (16)). Thus

$$C_{l_r} = \frac{\alpha}{B^2} C_{l_p}$$

The derivative C_{l_p} has been derived previously and is given in table II.

Derivatives C_{Y_r} and C_{n_r}.—When the wing yaws, the antisymmetrical pressure distribution which is indicated by equation (15) will produce unbalanced suction forces at the right and left wing tips and thereby give rise to lateral forces and yawing moments. In addition, skin friction will contribute a yawing moment.

It appears that a reasonable although approximate evaluation of the tip suction forces in yawing can be obtained by means of the correspondence of yawing with rolling as utilized previously in deriving equation (16). This procedure does not satisfy the Kutta-Joukowski requirement in the sideslip component of the stream velocity in yawing; however, this theoretical deviation is likely to be very small in the actual flow. On the basis of these considerations, the induced suction forces on the wing tips per unit yawing velocity will be related in the ratio α/B^2 to the corresponding induced suction forces per unit rolling velocity which were derived previously (section entitled "Derivatives C_{Y_p} and C_{n_p}"). The contributions of the tip suction forces to C_{Y_r} and $C_{n_{r_1}}$ are, therefore,

$$C_{Y_r} = \frac{\alpha}{B^2} C_{Y_p}$$

and

$$C_{n_{r_1}} = \frac{\alpha}{B^2} C_{n_p}$$

where C_{Y_p} and C_{n_p} are given in table II.

The effect of skin friction on the yawing moment due to yawing is

$$N_2 = \cos\alpha \int_{-h}^{h}\int_{0}^{c} C_{D_0}\frac{\rho}{2}\left[(V-ry)^2 + r\left(\frac{c}{2}-x\right)^2\right]\left[\left(x-\frac{c}{2}\right)\beta + y\right]dx\,dy$$

where the first bracketed term expresses the square of the resultant local velocity and β is the local angle of sideslip:

$$\beta = \frac{r\left(\frac{c}{2}-x\right)}{V}$$

Eliminating second-order terms and terms corresponding to symmetrical drag forces and converting N_2 to coefficient form yields

$$C_{n_{r_2}} = -\frac{C_{D_0}}{4ch^3}\int_{-h}^{h}\int_{0}^{c}\left[\left(x-\frac{c}{2}\right)^2 + 2y^2\right]dx\,dy$$

RESULTS AND DISCUSSION

As noted in the preceding analysis, the nondimensional stability derivatives which are presented in table II were derived with reference to principal body axes with the origin

at point $\left(\frac{c}{2}, 0, 0\right)$. These results may be transformed by means of the equations in the last column of table II to apply to stability axes with the origin at an arbitrary distance x_{cg} from the midchord point. The stability axes are shown in figures 2 (b) and are obtained by a rotation of the principal body axes (fig. 2 (a)) through an angle α; the origin is then shifted a distance x_{cg} along the new x-axis. The conversion to stability axes was obtained by means of the transformation formulas given in reference 16, with the omission of relatively unimportant terms compared to unity, such as α^2.

The formulas for the derivatives given in table II with reference to principal body axes are shown plotted in figures 4 and 5 against the parameter AB. (Derivative $-C_{X_u}$ and those derivatives equal to zero are omitted from the figures.) These curves show the variation of the stability derivatives with aspect ratio for constant Mach number. The variation with Mach number for constant aspect ratio is not

directly indicated, although it can be determined from the curves. These data are shown in figure 4 for the lateral stability derivatives and in figure 5 for the longitudinal stability derivatives. The data in figures 4 and 5 are to be used in conjunction with the transformation formulas presented in table II to evaluate the derivatives with respect to stability axes. In the evaluation of these derivatives, many of the terms are likely to be relatively small; therefore, the expressions will be noticeably simplified when such terms are neglected in the computations.

The results of the present investigation have been derived on the assumptions of zero thickness and small disturbances. Potential flow is assumed except in the case of C_{z_r} and C_{X_u} in which skin friction is considered. The practical effects of the Kutta-Joukowski requirements which are introduced at the wing tips in sideslip and yawing are not definitely known. On this basis, the data shown in figures 4 and 5 are expected to apply in general to thin wing sections for small steady motions, motions with small accelerations, or oscillatory motions of low frequency in which boundary-layer effects are not expected to be important. The applicability of the present theory to Mach numbers in the vicinity of unity, very high Mach numbers, or for very low aspect ratios is uncertain.

The data in figure 4 (a) show that at supersonic speeds the derivative $B^3C_{l_r}/\alpha$ is negative in contrast with the behavior

(a) Rolling-moment-coefficient derivatives. $C_{l_\beta} = C_{l_{1\beta}} + C_{l_{2\beta}}$
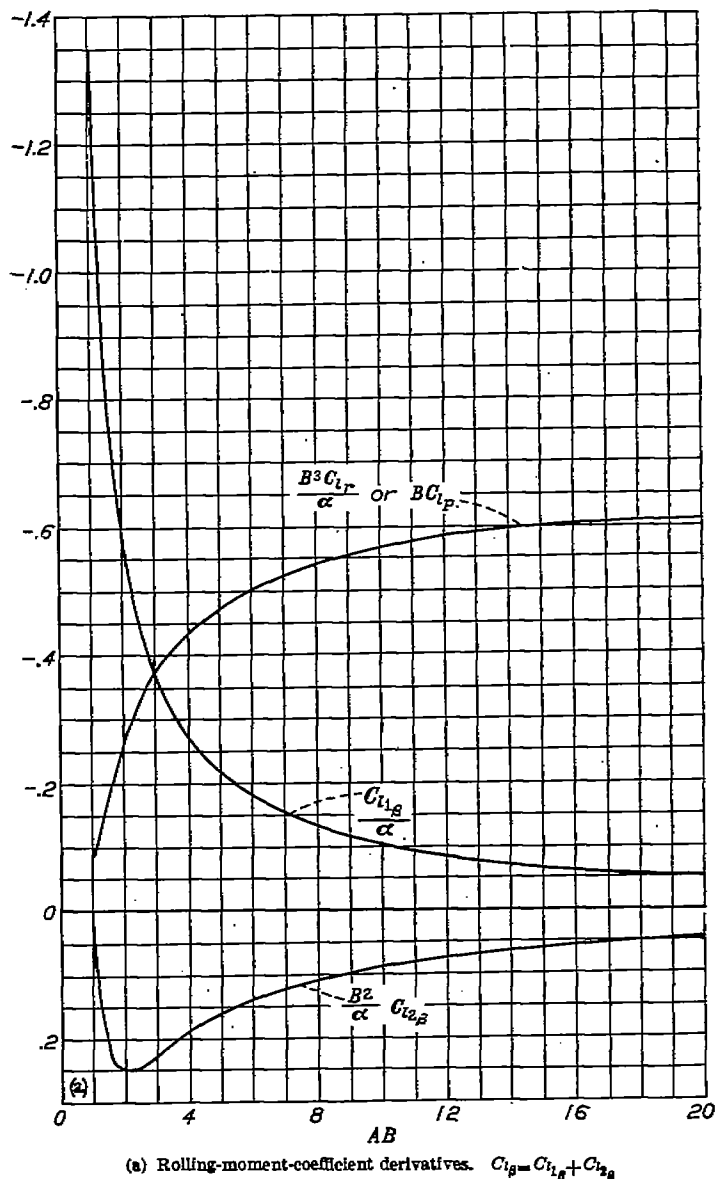
FIGURE 4.—Variation of supersonic lateral stability derivatives with aspect ratio-Mach number parameter. Derivatives with respect to principal body axes; thin flat rectangular wing; no dihedral. (See table II for conversion to stability axes.)
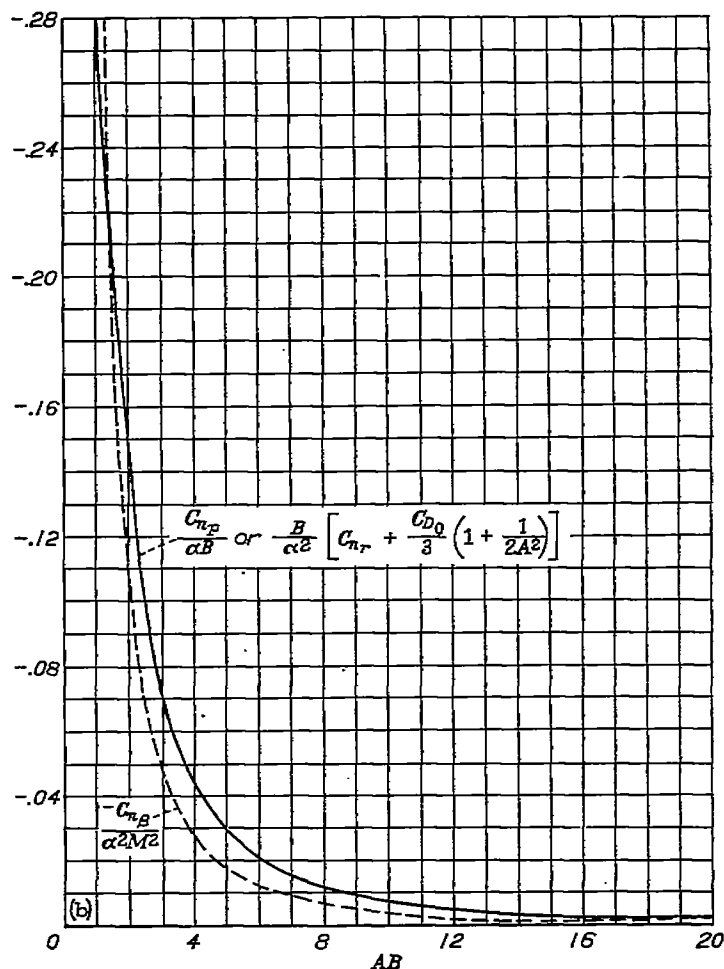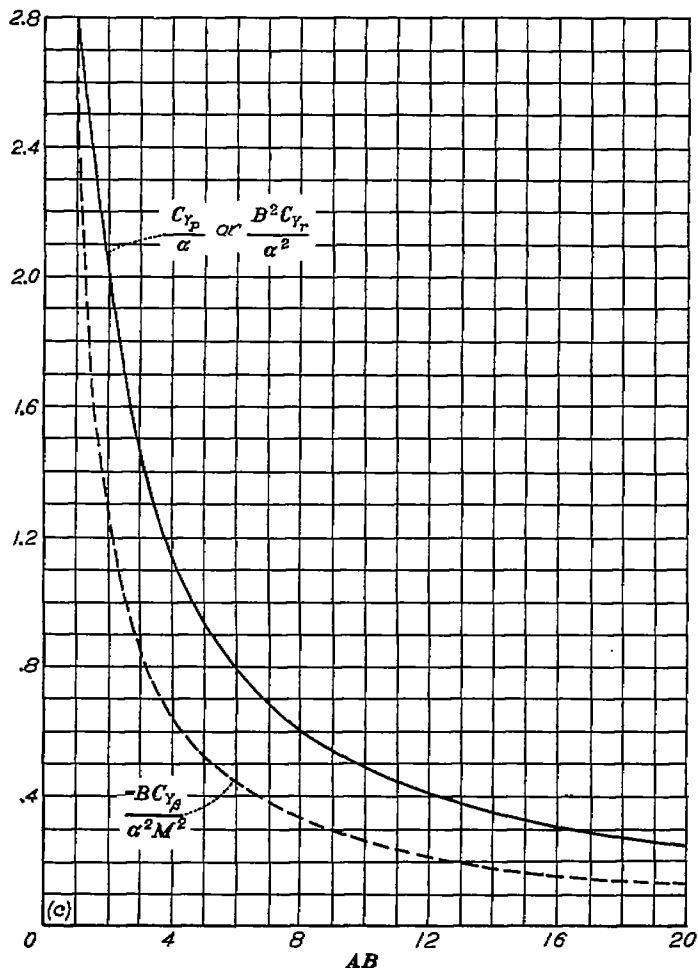

(b) Yawing-moment-coefficient derivatives.

FIGURE 4.—Continued.

(c) Side-force-coefficient derivatives.

Figure 4.—Concluded.

at subsonic speeds where positive values would be obtained. This phenomenon was pointed out for the infinitely long wing in reference 7 and its physical significance elaborated upon. For stability axes, the formula for C_{l_r}' (table II) indicates that another reversal in sign to a positive value occurs as the Mach number is increased beyond approximately 1.41 for typical rectangular wings. (Also see reference 7 for the infinitely long wing.)

The suction force at the leading edge of rectangular wings vanishes at supersonic speeds. This factor should have an important influence on the derivatives C_{n_p} and C_{n_r} as supersonic speeds are attained. In the case of C_{n_p}' (stability axes), the results of the present analysis indicate that at supersonic speeds the sign of C_{n_p}' will have positive values in many typical cases in contrast to negative values normally obtained at subsonic speeds. In the case of C_{n_r} or C_{n_r}', the loss of leading-edge suction tends to be compensated by the spanwise compressibility effects associated with supersonic speeds.

As noted previously in the analysis, the Kutta-Joukowski condition is unlikely to be satisfied along the trailing wing tip for a typically rounded wing tip at small angles of sideslip.

(a) $C_{z_{\dot{\alpha}}} = C_{z_{1_{\dot{\alpha}}}} + C_{z_{2_{\dot{\alpha}}}}.$

(b) $C_{z_u} = C_{z_{1_u}} + C_{z_{2_u}}.$
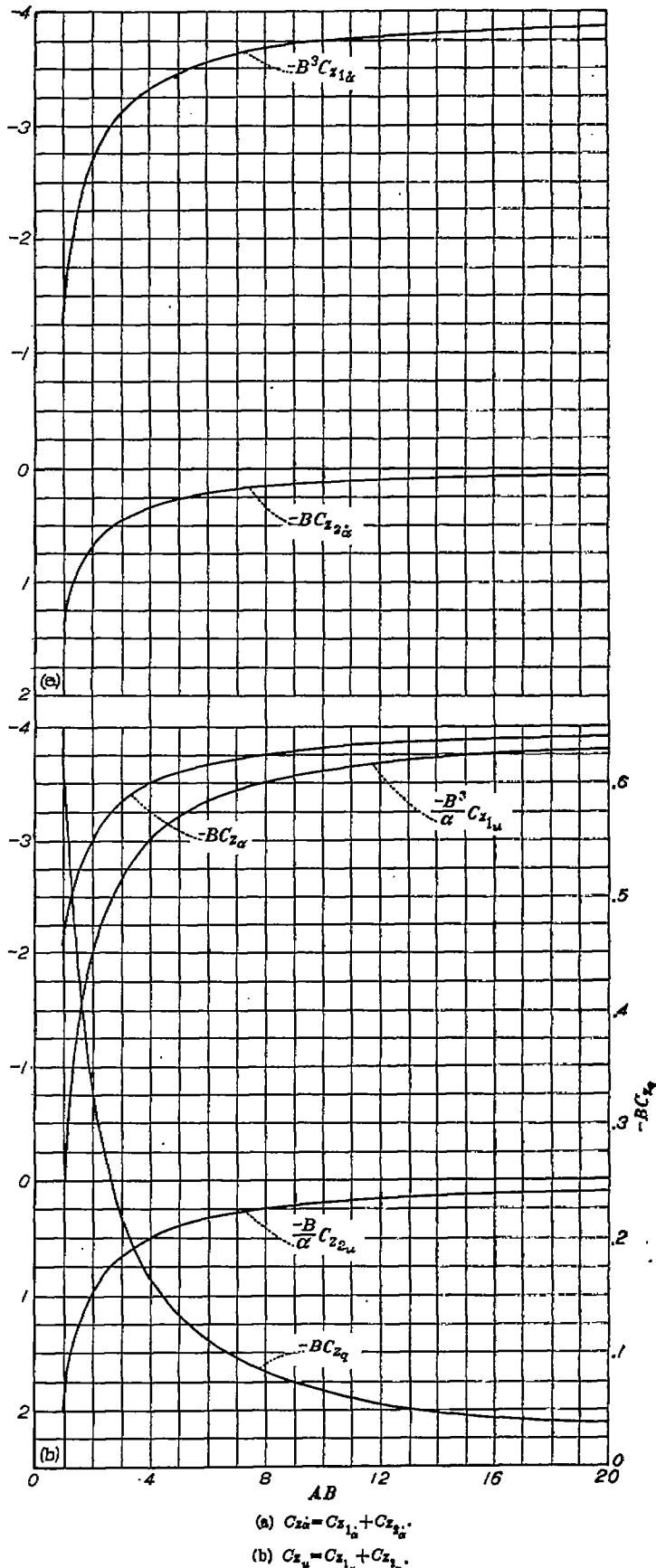
Figure 5.—Variation of supersonic longitudinal stability derivatives with aspect ratio-Mach number parameter. Derivatives with respect to principal body axes; thin flat rectangular wing. (See table II for conversion to stability axes.)

(c) $C_{m_{\dot\alpha}} = C_{m_{1_{\dot\alpha}}} + C_{m_{2_{\dot\alpha}}}$.

(d) $C_{m_q} = C_{m_{1_q}} + C_{m_{2_q}}$.
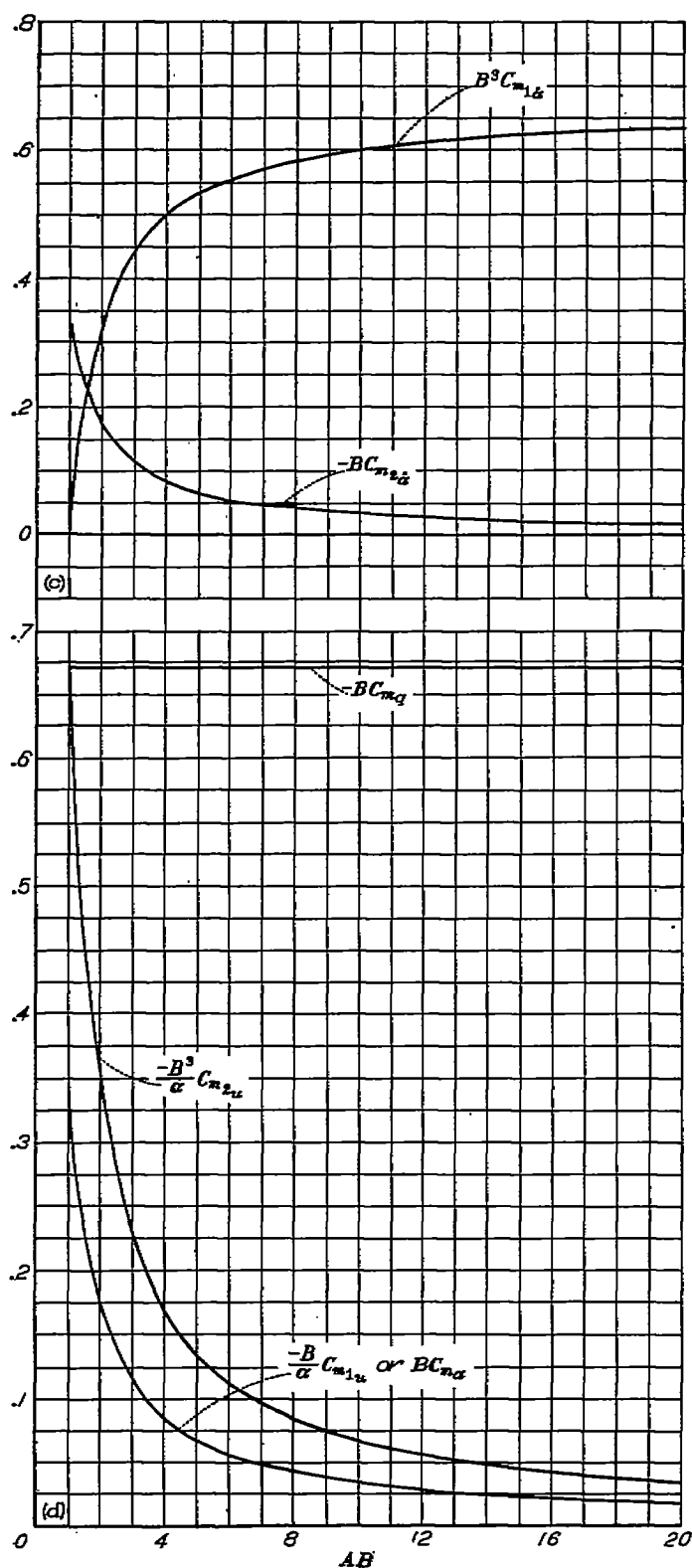
FIGURE 5.—Concluded.

Therefore, the results for C_{l_β} in figure 4 (a) are applicable where the Kutta-Joukowski condition along the wing trailing edge is not satisfied. In order to determine the effect on C_{l_β} of satisfying the Kutta-Joukowski condition along the trailing wing tip, the formula for C_{l_β} which meets this requirement was also obtained and is as follows:

$$C_{l_\beta} = \frac{\alpha}{B^2}\left(\frac{1}{AB} - \frac{3+2B^2}{3A^2B^2}\right)$$

A comparison of this formula with the data for C_{l_β} given in figure 4 (a) indicates that the effect of satisfying the Kutta-Joukowski condition along the trailing wing tip reduces negatively the values of C_{l_β} from those obtained by neglecting the Kutta-Joukowski condition. For example for $B=1$ and $AB=4$, when the Kutta-Joukowski condition along the trailing wing tip is neglected, $C_{l_\beta} = -0.083\alpha$; and when the Kutta-Joukowski condition is satisfied along the trailing wing tip, $C_{l_\beta} = 0.146\alpha$. Thus, it is expected that when the sideslip angle becomes large, the dihedral effect $-C_{l_\beta}$ should be reduced significantly because of the Kutta-Joukowski condition along the trailing wing tip.

The longitudinal stability derivatives in figure 5 refer to an axis whose origin is located at the midchord point. The data in figure 5 (c) for BC_{m_α} show that rectangular wings, with reference to this origin, have an increasingly unstable pitching moment with decreasing aspect ratio which corresponds to a forward shift in the aerodynamic center. For infinite aspect ratio, the aerodynamic center is located at the midchord point or $BC_{m_\alpha}=0$. If the aspect ratio is decreased to a value of 4 for a Mach number of 1.41, figure 5 indicates a forward shift of the aerodynamic center of 0.025 chord. With constant Mach number, the ratio $BC_{m_\alpha}/-BC_{z_\alpha}$ is obtained from figure 5 solely as a function of AB. These data indicate that with constant aspect ratio and increasing Mach number, the aerodynamic center will shift rearward. For an aspect ratio of 4, an increase in Mach number from 1.4 to 1.9 will shift the aerodynamic center rearward 0.01 chord.

The derivative $-C_{z_{\dot\alpha}}$ given in table II for infinite aspect ratio is negative which indicates negative damping or instability. The ratio $-C_{m_{\dot\alpha}}/-C_{z_{\dot\alpha}}$ from table II gives the location of the center of pressure of the resultant lift contributed by $\dot\alpha$. By taking this ratio for infinite aspect ratio, the center of pressure is found to be located at a point $\frac{2}{3}c$ behind the leading edge. The negative damping produced by $\dot\alpha$, therefore, gives an unstable pitching moment for center-of-gravity locations ahead of $x=\frac{2}{3}c$. These unstable tendencies caused by $\dot\alpha$ are minimized by the effects of finite span and the instability due to $C_{z_{\dot\alpha}}$ disappears entirely if $AB \leq \frac{M^2+1}{3}$.

CONCLUSIONS

A theoretical investigation has been made by means of the linearized theory to obtain formulas for the surface-velocity-potential functions, surface-pressure distributions, and stability derivatives for various motions at supersonic speeds for rectangular wings of zero thickness without dihedral. The investigation included steady and accelerating vertical and longitudinal motions and steady rolling, yawing, sideslipping, and pitching for Mach numbers and aspect ratios greater than those for which the Mach line from the leading edge of the tip section intersects the trailing edge of the opposite tip section.

The following significant conclusions have been obtained for this investigation:

1. At supersonic speeds for Mach numbers smaller than approximately 1.41, positive yawing generally results in a negative rolling moment in contrast to the behavior at subsonic speeds where a positive rolling moment is produced.

2. The attainment of supersonic speed produces a significant change in the positive direction of the yawing moment per unit rolling velocity.

3. For infinite aspect ratio, a constant vertical acceleration causes a negative damping in the vertical motion, and an unstable pitching moment for center-of-gravity locations ahead of the $\frac{2}{3}$-chord point. These unstable tendencies are minimized by the effects of finite span and the instability due to the rate of change of lift with vertical acceleration disappears entirely if $A\sqrt{M^2-1} \leq \frac{M^2+1}{3}$ where A is the aspect ratio and M is the Mach number.
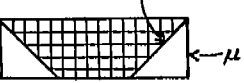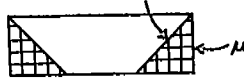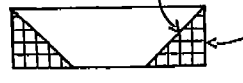
LANGLEY AERONAUTICAL LABORATORY,
  NATIONAL ADVISORY COMMITTEE FOR AERONAUTICS,
  LANGLEY FIELD, VA., *June 30, 1948.*

REFERENCES

1. Puckett, Allen E.: Supersonic Wave Drag of Thin Airfoils. Jour. Aero. Sci., vol. 13, no. 9, Sept. 1946, pp. 475–484.
2. Jones, Robert T.: Properties of Low-Aspect-Ratio Pointed Wings at Speeds below and above the Speed of Sound. NACA Rep. 835, 1946.
3. Brown, Clinton E.: Theoretical Lift and Drag of Thin Triangular Wings at Supersonic Speeds. NACA Rep. 839, 1946.
4. Evvard, John C.: Distribution of Wave Drag and Lift in the Vicinity of Wing Tips at Supersonic Speeds. NACA TN 1382, 1947.
5. Ribner, Herbert S.: The Stability Derivatives of Low-Aspect-Ratio Triangular Wings at Subsonic and Supersonic Speeds. NACA TN 1423, 1947.
6. Brown, Clinton E., and Adams, Mac C.: Damping in Pitch and Roll of Triangular Wings at Supersonic Speeds. NACA Rep. 892, 1948.
7. Ribner, Herbert S., and Malvestuto, Frank S., Jr.: Stability Derivatives of Triangular Wings at Supersonic Speeds. NACA TN 1572, 1948.
8. Moeckel, W. E.: Effect of Yaw at Supersonic Speeds on Theoretical Aerodynamic Coefficients of Thin Pointed Wings with Several Types of Trailing Edge. NACA TN 1549, 1948.
9. Jones, Arthur L., and Alksne, Alberta: The Damping Due to Roll of Triangular, Trapezoidal, and Related Plan Forms in Supersonic Flow. NACA TN 1548, 1948.
10. Evvard, John C.: A Linearized Solution for Time-Dependent Velocity Potentials near Three-Dimensional Wings at Supersonic Speeds. NACA TN 1699, 1948.
11. Evvard, John C.: Theoretical Distribution of Lift on Thin Wings at Supersonic Speeds (An Extension). NACA TN 1585, 1948.
12. Evvard, John C., and Turner, L. Richard: Theoretical Lift Distribution and Upwash Velocities for Thin Wings at Supersonic Speeds. NACA TN 1484, 1947.
13. Peirce, B. O.: A Short Table of Integrals. Third rev. ed., Ginn and Co., 1929.
14. Garrick, I. E., and Rubinow, S. I.: Flutter and Oscillating Air-Force Calculations for an Airfoil in Two-Dimensional Supersonic Flow. NACA Rep. 846, 1946.
15. Von Kármán, Th., and Burgers, J. M.: General Aerodynamic Theory—Perfect Fluids. Theory of Airplane Wings of Infinite Span. Vol. II of Aerodynamic Theory, div. E, ch. II, sec. 10, W. F. Durand, ed., Julius Springer (Berlin), 1935, pp. 48–53.
16. Glauert, H.: A Non-Dimensional Form of the Stability Equations of an Aeroplane. R. & M. No. 1093, British A.R.C., 1927.

[Thin flat rectangular wing; no dihedral; $AB \geqq 2$; axes are shown in figs. 1 and 2]

(a) Wing / Motion	Velocity potential on upper surface, ϕ		Pressure-difference coefficient between upper and lower surfaces, Δc_P	
	(b)		(b)	
Vertical, w	$\dfrac{V\alpha x}{B}$	$\dfrac{V\alpha}{\pi}\left[\dfrac{x}{B}\cos^{-1}\left(\dfrac{2y_aB}{x}+1\right)+2\sqrt{-y_a\left(y_a+\dfrac{x}{B}\right)}\right]$	$\dfrac{4\alpha}{B}$	$\dfrac{4\alpha}{\pi B}\cos^{-1}\left(\dfrac{2y_aB}{x}+1\right)$
Accelerated vertical, $\dot{w}$	$\dfrac{V\dot{\alpha}x}{B}\left(t-\dfrac{M^2x}{2B^2V}\right)$	$\dfrac{\dot{\alpha}}{B\pi}\left\{\left[2BVt+\dfrac{M^2(2y_aB-x)}{3B}\right]\sqrt{-y_a\left(y_a+\dfrac{x}{B}\right)}+\left(Vxt-\dfrac{M^2x^2}{2B^2}\right)\cos^{-1}\left(\dfrac{2y_aB}{x}+1\right)\right\}$	$\left(-\dfrac{4x\dot{\alpha}}{VB^3}\right)_{t\to0}$	$\left\{\dfrac{4\dot{\alpha}}{\pi B^2V}\left[-\dfrac{x}{B}\cos^{-1}\left(\dfrac{2y_aB}{x}+1\right)+2B^2\sqrt{-y_a\left(y_a+\dfrac{x}{B}\right)}\right]\right\}_{t\to0}$
Pitching, q	$\dfrac{qx(x-c)}{2B}$	$\dfrac{q}{\pi}\left[\dfrac{x}{2B}(x-c)\cos^{-1}\left(\dfrac{2y_aB}{x}+1\right)+\left(\dfrac{5x+2y_aB-3c}{3}\right)\sqrt{-y_a\left(y_a+\dfrac{x}{B}\right)}\right]$	$\dfrac{4q\left(x-\dfrac{c}{2}\right)}{BV}$	$\dfrac{4q}{\pi V}\left[\dfrac{\left(x-\dfrac{c}{2}\right)}{B}\cos^{-1}\left(\dfrac{2y_aB}{x}+1\right)+2\sqrt{-y_a\left(y_a+\dfrac{x}{B}\right)}\right]$
Rolling, p	$\dfrac{pyx}{B}$	$\dfrac{2p}{\pi}\left[\dfrac{x}{B}(y_a+h)\sin^{-1}\sqrt{\dfrac{-y_aB}{x}}-\dfrac{1}{3}\left(\dfrac{2x}{B}-y_a-3h\right)\sqrt{-y_a\left(y_a+\dfrac{x}{B}\right)}\right]$	$\dfrac{4py}{BV}$	$\dfrac{8p}{\pi BV}\left[(y_a+h)\sin^{-1}\sqrt{\dfrac{-y_aB}{x}}-\sqrt{-y_a\left(y_a+\dfrac{x}{B}\right)}\right]$
Combined side-slipping, v, and vertical, w	$\dfrac{V\alpha x}{B}$	(c) $\dfrac{V\alpha}{\pi}\left\{\dfrac{x}{\sqrt{B^2-\beta^2}}\cos^{-1}\left[\dfrac{2y_a(B-\beta)}{x(1+B\beta)}+1\right]+\dfrac{2}{1+B\beta}\sqrt{\dfrac{-y_a}{B+\beta}}[y_a(B-\beta)+x(1+B\beta)]\right\}$	(c) $\dfrac{4\alpha}{B}$	(c) $\dfrac{4\alpha}{\pi B}\left\{\dfrac{B}{\sqrt{B^2-\beta^2}}\cos^{-1}\left[\dfrac{2y_a(B-\beta)}{x(1+B\beta)}+1\right]+\dfrac{2B\beta}{1+B\beta}\sqrt{\dfrac{1}{B+\beta}}\left[\dfrac{x(1+B\beta)}{-y_a}-(B-\beta)\right]\right\}$
Yawing, r	$\dfrac{\alpha M^2 ryx}{B^3}$		$\dfrac{4\alpha ry}{B^3V}$	(d) $\dfrac{8\alpha r}{\pi B^3V}\left[(y_a+h)\sin^{-1}\sqrt{\dfrac{-y_aB}{x}}-\sqrt{-y_a\left(y_a+\dfrac{x}{B}\right)}\right]$

a Crosshatching indicates region where formulas are applicable.
b Also infinite aspect ratio.

c Formula applies to right half-wing; for left half-wing, replace β by $-\beta$.
d Not established rigorously; see text.

TABLE II.—STABILITY DERIVATIVES OF THIN FLAT RECTANGULAR WINGS WITHOUT DIHEDRAL AT SUPERSONIC SPEEDS

Principal body axes $\left(\text{origin at point }\left(\frac{c}{2},0,0\right)\right)$		Stability axes $\left(\text{origin at distance }x_{cs}\text{ measured positive ahead of midchord point }\left(\frac{c}{2}-x_{cs},0,0\right)\right)$	
Stability derivative	Formula	Stability derivative	Formula
Lateral			
C_{l_p}	$-\frac{1}{B}\left(\frac{2}{3}-\frac{1}{AB}+\frac{1}{3A^2B^2}+\frac{1}{12A^3B^3}\right)$	C_{l_p}'	$C_{l_p}+\alpha\left[C_{l_r}+C_{n_p}-\frac{x_{cs}}{cA}\left(2C_{l_\beta}+C_{Y_p}\right)\right]$
C_{l_β}	$\frac{\alpha}{B^2}\left(\frac{1-B^2}{AB}-\frac{3+B^2}{3A^2B^2}\right)$	C_{l_β}'	$C_{l_\beta}+\alpha\left(C_{n_\beta}-\frac{x_{cs}}{cA}C_{Y_\beta}\right)$
C_{l_r}	$-\frac{\alpha}{B^3}\left(\frac{2}{3}-\frac{1}{AB}+\frac{1}{3A^2B^2}+\frac{1}{12A^3B^3}\right)$	C_{l_r}'	$C_{l_r}-\frac{2x_{cs}}{cA}C_{l_\beta}-\alpha\left[C_{l_p}-C_{n_r}+\frac{x_{cs}}{cA}\left(C_{Y_r}+2C_{n_\beta}\right)-\frac{2x_{cs}^2}{c^2A^2}C_{Y_\beta}\right]-\alpha^2C_{n_p}$
C_{n_p}	$-\frac{8B\alpha}{3\pi}\left(\frac{1}{A^2B^2}-\frac{2}{3A^3B^3}\right)$	C_{n_p}'	$C_{n_p}-\frac{x_{cs}}{cA}C_{Y_p}-\alpha\left[C_{l_p}-C_{n_r}+\frac{x_{cs}}{cA}\left(C_{Y_r}+2C_{n_\beta}\right)-\frac{2x_{cs}^2}{c^2A^2}C_{Y_\beta}\right]-\alpha^2\left(C_{l_r}-\frac{2\bar{x}_{cs}}{cA}C_{l_\beta}\right)$
C_{n_β}	$\frac{4\alpha^2M^2}{3\pi A^2B^3}$	C_{n_β}'	$C_{n_\beta}-\frac{x_{cs}}{cA}C_{Y_\beta}-\alpha C_{l_\beta}$
C_{n_r}	$-\frac{8\alpha^2}{3\pi B}\left(\frac{1}{A^2B^2}-\frac{2}{3A^3B^3}\right)-\frac{C_{D_0}}{3}\left(1+\frac{1}{2A^2}\right)$	C_{n_r}'	$C_{n_r}-\frac{x_{cs}}{cA}\left(C_{Y_r}+2C_{n_\beta}\right)+\frac{2x_{cs}^2}{c^2A^2}C_{Y_\beta}+\alpha\left[-C_{l_r}-C_{n_p}+\frac{x_{cs}}{cA}\left(2C_{l_\beta}+C_{Y_p}\right)\right]+\alpha^2C_{l_p}$
C_{Y_p}	$\frac{16\alpha}{\pi}\left(\frac{1}{AB}-\frac{4}{9A^2B^2}\right)$	C_{Y_p}'	$C_{Y_p}+\alpha\left(C_{Y_r}-\frac{2x_{cs}}{cA}C_{Y_\beta}\right)$
C_{Y_β}	$-\frac{8\alpha^2M^2}{\pi AB^2}$	C_{Y_β}'	C_{Y_β}
C_{Y_r}	$\frac{16\alpha^2}{B^2\pi}\left(\frac{1}{AB}-\frac{4}{9A^2B^2}\right)$	C_{Y_r}'	$C_{Y_r}-\frac{2x_{cs}}{cA}C_{Y_\beta}-\alpha C_{Y_p}$
Longitudinal			
C_{m_α}	$\frac{1}{3AB^2}$	C_{m_α}'	$C_{m_\alpha}-\alpha C_{m_u}+\frac{x_{cs}}{c}\left(C_{Z_\alpha}-\alpha C_{Z_u}\right)$
C_{m_u}	$-\frac{\alpha}{3AB^4}(M^2+1)$	C_{m_u}'	$C_{m_u}+\alpha C_{m_\alpha}+\frac{x_{cs}}{c}\left(\alpha C_{Z_\alpha}+C_{Z_u}\right)$
C_{m_q}	$-\frac{2}{3B}$	C_{m_q}'	$C_{m_q}+2\left(\frac{x_{cs}}{c}\right)^2C_{Z_\alpha}$
$C_{m_{\dot\alpha}}$	$\frac{1}{3B^3}\left(2-\frac{2+B^2}{AB}\right)$	$C_{m_{\dot\alpha}}'$	$C_{m_{\dot\alpha}}+\frac{x_{cs}}{c}C_{Z_{\dot\alpha}}$
$C_{m_{\dot u}}$	0	$C_{m_{\dot u}}'$	$\alpha\left(C_{m_{\dot\alpha}}+\frac{x_{cs}}{c}C_{Z_{\dot\alpha}}\right)$
$-C_{Z_\alpha}$	$\frac{4}{B}\left(1-\frac{1}{2AB}\right)$	$-C_{Z_\alpha}'$	$\alpha C_{Z_u}-C_{Z_\alpha}$
$-C_{Z_u}$	$\frac{2\alpha}{AB^4}(M^2+1-2AB)$	$-C_{Z_u}'$	$-C_{Z_u}+\alpha(C_{X_u}-C_{Z_\alpha})$
$-C_{Z_q}$	$\frac{2}{3AB^2}$	$-C_{Z_q}'$	$-C_{Z_q}-\frac{2x_{cs}}{c}C_{Z_\alpha}$
$-C_{Z_{\dot\alpha}}$	$\frac{1}{B^3}\left(-4+\frac{8+4B^2}{3AB}\right)$	$-C_{Z_{\dot\alpha}}'$	$-C_{Z_{\dot\alpha}}$
$-C_{Z_{\dot u}}$	0	$-C_{Z_{\dot u}}'$	$-\alpha C_{Z_{\dot\alpha}}$
$-C_{X_\alpha}$	0	$-C_{X_\alpha}'$	$\alpha(C_{X_u}-C_{Z_\alpha})+\alpha^2C_{Z_u}$
$-C_{X_u}$	$2C_{D_0}$	$-C_{X_u}'$	$-C_{X_u}-\alpha C_{Z_u}-\alpha^2C_{Z_\alpha}$
$-C_{X_q}$	0	$-C_{X_q}'$	$-\alpha\left(C_{Z_q}+\frac{2x_{cs}}{c}C_{Z_\alpha}\right)$
$-C_{X_{\dot\alpha}}$	0	$-C_{X_{\dot\alpha}}'$	$-\alpha C_{Z_{\dot\alpha}}$
$-C_{X_{\dot u}}$	0	$-C_{X_{\dot u}}'$	$-\alpha^2C_{Z_{\dot\alpha}}$